

The studies of structure, thermodynamic properties and theoretical analyses of 2-[(4-nitro-benzoyl)-hydrazone]-propionic acid

Yongliang Liu ^a, Youying Di ^a, Yanqing Di ^a, Chengfang Qiao ^a, Fengying Chen ^a, Fei Yuan ^a, Kefen Yue ^b, Chunsheng Zhou ^{a,*}

^a College of Chemical Engineering and Modern Materials, Shaanxi Key Laboratory of Comprehensive Utilization of Tailings Resources, Shangluo University, Shangluo, 726000, PR China

^b Key Laboratory of Synthetic and Natural Functional Molecule Chemistry of the Ministry of Education, Shaanxi Key Laboratory of Physico-Inorganic Chemistry, College of Chemistry & Materials Science, Northwest University, Xi'an, 710069, PR China

ARTICLE INFO

Article history:

Received 20 October 2018

Received in revised form

12 February 2019

Accepted 13 February 2019

Available online 14 February 2019

Keywords:

2-[(4-nitro-benzoyl)-hydrazone]-propionic acid

Low-temperature heat capacity

Standard molar enthalpy of formation

Optimized structure

Frontier molecular orbital

Molecular electrostatic potential

ABSTRACT

In this work, 2-[(4-nitro-benzoyl)-hydrazone]-propionic acid ($C_{10}H_9O_5N_3$), a Schiff base compound was synthesized and structurally characterized. The low-temperature heat capacities of $C_{10}H_9O_5N_3$ were measured with a small sample precision automated adiabatic calorimeter from 78 to 400 K. The curve of experimental heat capacity versus reduced temperature of $C_{10}H_9O_5N_3$ has been fitted with a polynomial equation by the least-squares method, the fitting result shows that the structure of $C_{10}H_9O_5N_3$ is stable in the whole temperature region. The smoothed heat capacities and thermodynamic functions of the title compound were calculated by the polynomial equations with an interval of 5 K. The constant-volume combustion energy for $C_{10}H_9O_5N_3$ was determined by an RBC-II precision rotating bomb combustion calorimeter. According to one designed thermochemical cycle, and combined with some other auxiliary thermodynamic data, the standard molar enthalpy of formation of the $C_{10}H_9O_5N_3$ was calculated, and $\Delta_f H_m^\circ (C_{10}H_9O_5N_3, s) = -(667.31 \pm 11.02) \text{ kJ} \cdot \text{mol}^{-1}$. In addition, optimized structure, frontier molecular orbitals, and molecular electrostatic potential of $C_{10}H_9O_5N_3$ were analyzed by using B3LYP calculation with 6-31G (d,p) basis set.

© 2019 Elsevier B.V. All rights reserved.

1. Introduction

As a branch of Schiff base, acylhydrazones have received extensive attention because of their biological and therapeutic properties, such as antimicrobial activity [1–3], anticancer activity [4–6], insecticidal activity [7–9], antitubercular activity [10–12] and antioxidant activity [13–15]. So they have been extensively investigated and used in drug exploitation in the past few decades. Moreover, acylhydrazones behave as chelating ligands due to their N and O atoms. So various acylhydrazone complexes with stronger biological activities have been synthesized [16–21].

As we know, the thermodynamic properties play very important roles in chemistry, chemical simulation, chemical engineering, industrial applications [22–25]. The heat capacity and enthalpy are the most important thermodynamic properties, not only because they can be used to calculate enthalpy changes, entropy and Gibbs

free energy, equilibrium constant and so on, but also in calculating thermodynamic parameters of the certain compounds [26]. For example, the T_{trans} , ΔH_{trans} and ΔS_{trans} for $(n-C_{18}H_{37}NH_3)_2CdCl_4$ have been derived based on heat-capacity measurements [27]. The $\Delta_f H_m^\circ$ and $\Delta_f H_m^\circ$ of $Ba(C_7H_5O_2)_2(s)$ have been measured from the dissolution enthalpies of the reactants combined with some auxiliary thermodynamic data [28]. In addition, with the improvement of quantum chemistry and the increasing development of computing method, the density functional theory (DFT) is becoming more and more important in the field of organic chemistry. It has been a valuable tool in predicting and analyzing the kinetic stability and the chemically active sites of the molecule [29]. To the best of our knowledge, frontier molecular orbitals (HOMO and LUMO) can be used for analyzing electronic structure, charge transfer and reaction mechanism of molecular [30,31]. Molecular electrostatic potential (MEP) analysis is used as a theoretical method to predict reaction sites, intermolecular binding patterns and thermodynamic properties of molecular, etc [32,33]. However, as yet extensive literature survey reveals that the thermodynamic

* Corresponding author.

E-mail address: liumaliang@163.cm (C. Zhou).

properties and theoretical analyses of acylhydrazones are rarely, which provide a chance for us to carry on this research. The expected results of the study can provide theoretical basis for the pharmacological research and industrial application of the acylhydrazones.

In this study, the 2-[(4-nitro-benzoyl)-hydrazone]-propionic acid ($C_{10}H_9O_5N_3$, Scheme 1) was synthesized, and the structure was characterized by X-ray diffractometer (XRD), IR, and elemental analysis. The low-temperature heat capacities and the standard molar enthalpy of formation of the $C_{10}H_9O_5N_3$ were measured by adiabatic calorimetry and combustion calorimetry, respectively. The optimized molecular structure, frontier molecular orbitals (HOMO and LUMO), and molecular electrostatic potential (MEP) analysis of the title compound were investigated by using the DFT method at the B3LYP/6-31G(d,p) level.

2. Experimental section

2.1. Preparation of $C_{10}H_9O_5N_3$

4-nitro-benzoylhydrazide and pyruvic acid were commercially available and used as received. $C_{10}H_9O_5N_3$ was synthesized by literature method with minor modifications [34]. 4-nitro-benzoylhydrazide (2.325 g, 10 mmol) was dissolved in absolute ethyl alcohol (30 mL), and stirred until entirely dissolved. Then, pyruvic acid (1.232 g, 14 mmol) was slowly added to the above transparent solution via a dropping funnel. The mixture solution was heated under reflux for 2 h. Finally, the precipitate was filtered in vacuo to give a pale yellow powder. The powder was recrystallized from ethanol, and the yellow product was obtained. Yield: 71.62%. Anal. calcd for $C_{10}H_9N_3O_5$: C, 47.81; H, 3.61; N, 16.73. Found: C, 47.92; H, 3.67; N, 16.64. IR (KBr, cm^{-1}): 1690, 1570, 1530, 1490, 1270, 1030, 854, 791, 715.

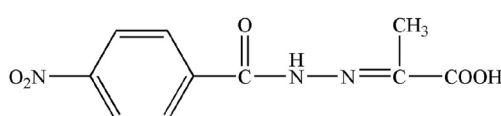
2.2. Preparation of the compound [$C_{10}H_9O_5N_3 \cdot H_2O$]_n

The $C_{10}H_9O_5N_3$ (0.10 g, 0.40 mmol) was dissolved in mixed solution of C_2H_5OH and H_2O ($V_{\text{ethanol}}:V_{\text{water}} = 1:1$, 20 mL). Then the solution was filtered, and the filtrate was naturally evaporated at room temperature. After three days, the yellow columnar crystals were collected, and dried in the air (Yield: 52.21%). The crystal structure of above crystal was determined by the single crystal X-ray diffraction. Crystal data: [$C_{10}H_9O_5N_3 \cdot H_2O$]_n, Monoclinic, $P 2_1$, $a = 6.5892(17)$ Å, $b = 11.781(3)$ Å, $c = 7.590(2)$ Å, $V = 587.8(3)$ Å³, $Z = 2$. The asymmetric unit of compound contains one $C_{10}H_9O_5N_3$ molecule and one lattice H_2O molecule (Fig. S1). The detailed crystallographic data were summarized in Table S1. Selected bond lengths and angles were listed in Tables S2-S3, Supporting Information. CCDC number is 1578867 for compound [$C_{10}H_9O_5N_3 \cdot H_2O$]_n.

3. Results and discussion

3.1. Low-temperature heat capacities

The experimental results of low-temperature heat capacities of the sample are listed in Table 1 and plotted in Fig. 1. As can be seen



Scheme 1. Structure of $C_{10}H_9O_5N_3$.

from Fig. 1, the whole heat capacity curve increases with the increase of temperature from 78 to 400 K, and no anomaly, which indicates that the structure of the substance is stable in the whole temperature region. All points of experimental molar heat capacities ($C_{p,m}$) versus reduced temperatures (X) were fitted with a polynomial equation by means of the least-squares method. The correlation coefficient for the fitting R^2 equals 0.99998, the fitting equation as follows:

$$C_{p,m}/(J \cdot K^{-1} \cdot mol^{-1}) = 252.947 + 198.770X - 71.519X^2 - 15.513X^3 + 22.146X^4 \quad (1)$$

In which $X = (T-239)/161$ is the reduced temperature, $X = [T - (T_{\max} + T_{\min})/2]/[(T_{\max} - T_{\min})/2]$, T is the experimental temperature; T_{\max} and T_{\min} are the upper and lower limits of the temperature region, respectively.

Smoothed values of the molar heat capacities were obtained based on the fitted polynomial equation (1). The relative deviations between the experimental values and the smoothed values are $\pm 0.4\%$ except for few points. The other fundamental thermodynamic functions of the sample relative to the standard reference temperature 298.15 K can be calculated according to the thermodynamic equations (2)–(4). The results are tabulated in Table 2 at the intervals of 5 K.

$$(H_T - H_{298.15}) = \int_{298.15}^T C_{p,m} dT \quad (2)$$

$$(S_T - S_{298.15}) = \int_{298.15}^T C_{p,m} \cdot T^{-1} dT \quad (3)$$

$$(G_T - G_{298.15}) = \int_{298.15}^T C_{p,m} dT - T \cdot \int_{298.15}^T C_{p,m} \cdot T^{-1} dT \quad (4)$$

3.2. Standard molar enthalpy of formation

The constant-volume energy of combustion of $C_{10}H_9O_5N_3$ was determined using an RBC-II precision rotating bomb combustion calorimeter. The $\Delta_c U$ of the $C_{10}H_9O_5N_3$ can be calculated from Eq (5). The experimental results are listed in Table 3.

$$-\Delta_c U/J \cdot g^{-1} = (\varepsilon_{\text{calor}} \cdot \Delta T - Q_{\text{Ni}} - Q_{\text{HNO}_3})/W \quad (5)$$

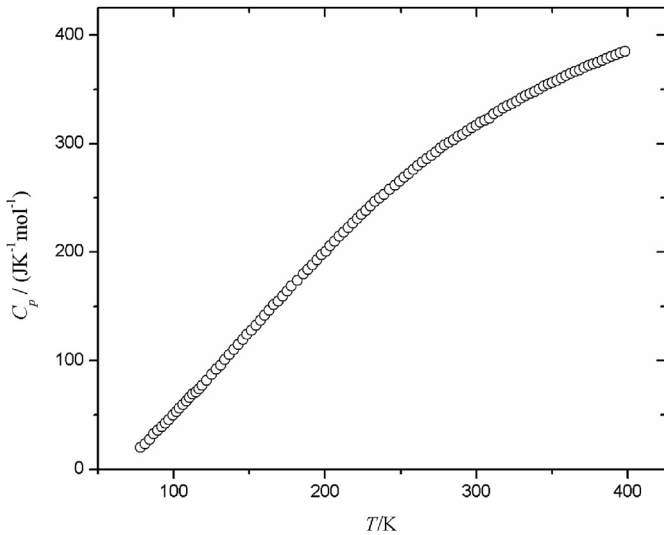
where $\Delta_c U/(J \cdot g^{-1})$ is the constant-volume energy of combustion of the sample; $\varepsilon_{\text{calor}}/(J \cdot K^{-1})$ is the energy equivalent of the oxygen-bomb calorimeter; $\Delta T/K$ is the corrected temperature rise; W/g is the mass of the sample. $\sigma_a = \sqrt{\sum_{i=1}^n (x_i - \bar{x})^2 / n(n-1)}$, in which n is the experimental number; x_i is a single value obtained from a series of measurements; \bar{x} is the mean value of the results.

At $T = 298.15$ K, the pressure quotient of the constant-volume energy of combustion: $(\partial u / \partial p)_T = -0.2 \text{ J} \cdot \text{g}^{-1} \cdot \text{MPa}^{-1}$ [35]. Considering that the pressure was corrected from 2.50 to 0.1 MPa, $\Delta P = -2.49 \text{ MPa}$, the change of the constant-volume energy of combustion of the sample $\Delta(\Delta_c U)$ was calculated to $0.50 \text{ J} \cdot \text{g}^{-1}$. Therefore, the standard ($p^\circ = 0.1 \text{ MPa}$) constant-volume energy of combustion for $C_{10}H_9O_5N_3$ was corrected to be $\Delta_c U^\circ = -(18161.35 \pm 49.79) \text{ J} \cdot \text{g}^{-1} + 0.50 \text{ J} \cdot \text{g}^{-1} = -(18160.85 \pm 49.79) \text{ J} \cdot \text{g}^{-1}$, and $\Delta_c U_m^\circ = -(4558.37 \pm 12.50) \text{ kJ} \cdot \text{mol}^{-1}$.

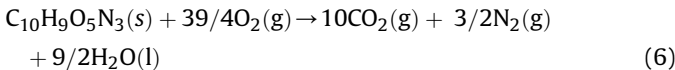
The standard molar enthalpy of combustion, $\Delta_c H_m^\circ$, of $C_{10}H_9O_5N_3$

Table 1Experimental molar heat capacities of $C_{10}H_9O_5N_3$.

T/K	$C_p, m/(J \cdot K^{-1} \cdot mol^{-1})$	T/K	$C_p, m/(J \cdot K^{-1} \cdot mol^{-1})$	T/K	$C_p, m/(J \cdot K^{-1} \cdot mol^{-1})$
78.112	20.258	177.83	168.51	290.95	308.55
81.065	23.481	181.85	173.58	293.92	311.76
83.911	27.395	185.85	179.79	296.88	314.49
86.661	32.459	188.80	183.94	299.84	316.61
89.325	35.682	191.76	188.08	302.78	319.44
91.908	38.905	194.68	192.91	305.76	321.57
94.422	42.358	197.62	197.52	308.78	323.45
96.867	45.581	200.56	200.74	311.78	327.50
99.252	49.955	203.51	205.58	314.77	329.83
101.58	53.178	206.47	209.72	317.75	332.40
103.86	56.401	209.40	214.55	320.71	334.89
106.08	59.624	212.34	218.24	323.66	336.86
108.26	62.847	215.28	222.38	326.60	338.99
110.40	65.839	218.24	226.75	329.57	341.64
112.50	69.062	221.21	230.67	332.59	344.05
114.56	71.364	224.16	234.35	335.58	346.05
116.59	74.127	227.11	238.27	338.57	347.98
118.58	77.350	230.07	242.64	341.55	350.35
121.67	81.724	233.03	246.78	344.52	352.80
125.21	87.249	236.01	250.01	347.47	354.56
128.08	91.853	238.98	253.19	350.42	356.05
130.97	95.766	242.73	257.66	353.40	358.02
133.86	100.83	246.48	261.43	356.42	360.55
136.77	105.44	249.44	265.11	359.43	362.51
139.69	110.27	252.37	268.68	362.42	364.36
142.62	114.64	255.33	272.34	365.41	366.29
145.56	119.48	258.33	276.03	368.39	367.93
148.50	124.08	261.31	279.64	371.36	370.14
151.43	128.00	264.26	282.78	374.32	371.95
154.34	132.60	267.20	285.99	377.27	373.23
157.26	136.97	270.17	288.88	380.21	374.92
160.19	141.58	273.17	291.97	383.19	376.65
163.14	146.41	276.16	295.79	386.21	378.53
166.09	151.25	279.13	298.52	389.22	380.38
169.03	154.70	282.08	300.80	392.21	381.75
171.95	159.53	285.00	303.09	395.20	383.35
174.88	164.14	287.96	306.71	398.19	385.15

**Fig. 1.** The curve of experimental molar heat capacities of $C_{10}H_9O_5N_3$.

could be derived from the $\Delta_c U_m^\circ$ at $T = 298.15$ K by means of Eq (6) - Eq (8):



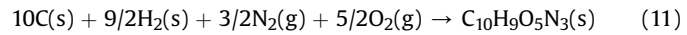
$$\Delta_c H_m^\circ = \Delta_c U_m^\circ + \Delta n RT \quad (7)$$

$$\Delta n = \sum_{n_i} (\text{products, g}) - \sum_{n_j} (\text{reactants, g}) \quad (8)$$

where $\sum n_i$ and $\sum n_j$ are the sum of the stoichiometric coefficients of the gaseous products and gaseous reactants, respectively.

$$\Delta_c H_m^\circ = -(4554.03 \pm 12.50) kJ \cdot mol^{-1}$$

In accordance with Hess' law, Eq (11) can be derived by the following formula: Eq (11) = 10Eq (9) + 9/2Eq (10) - Eq (6)



The standard molar enthalpy of formation, $\Delta_f H_m^\circ$, of $C_{10}H_9O_5N_3$ could be derived to be:

$$\Delta_f H_m^\circ(C_{10}H_9O_5N_3, s) = 10\Delta_f H_m^\circ(CO_2, g) + 9/2\Delta_f H_m^\circ(H_2O, l) - \Delta_c H_m^\circ(C_{10}H_9O_5N_3, s)$$

Table 2Smoothed molar heat capacities and thermodynamic functions of $C_{10}H_9O_5N_3$.

T (K)	$C_p/(J \cdot K^{-1} \cdot mol^{-1})$	$H_T - H_{298.15}/(kJ \cdot mol^{-1})$	$S_T - S_{298.15}/(J \cdot K^{-1} \cdot mol^{-1})$	$G_T - G_{298.15}/(kJ \cdot mol^{-1})$
80	22.901	-39.104	-192.558	-23.700
85	29.499	-38.973	-190.973	-22.741
90	36.279	-38.809	-189.095	-21.790
95	43.224	-38.610	-186.949	-20.850
100	50.316	-38.376	-184.552	-19.921
105	57.539	-38.107	-181.922	-19.005
110	64.877	-37.801	-179.077	-18.102
115	72.313	-37.458	-176.029	-17.215
120	79.832	-37.078	-172.793	-16.342
125	87.420	-36.659	-169.380	-15.487
130	95.061	-36.203	-165.803	-14.649
135	102.744	-35.709	-162.071	-13.829
140	110.453	-35.176	-158.196	-13.028
145	118.176	-34.604	-154.185	-12.247
150	125.902	-33.994	-150.048	-11.487
155	133.617	-33.345	-145.794	-10.747
160	141.311	-32.658	-141.431	-10.029
165	148.973	-31.932	-136.965	-9.333
170	156.592	-31.168	-132.404	-8.660
175	164.159	-30.366	-127.756	-8.009
180	171.664	-29.527	-123.026	-7.382
185	179.099	-28.650	-118.221	-6.779
190	186.454	-27.736	-113.347	-6.200
195	193.723	-26.785	-108.409	-5.646
200	200.898	-25.799	-103.414	-5.116
205	207.971	-24.777	-98.366	-4.612
210	214.937	-23.719	-93.271	-4.132
215	221.790	-22.627	-88.133	-3.679
220	228.523	-21.502	-82.957	-3.251
225	235.133	-20.342	-77.747	-2.849
230	241.615	-19.150	-72.508	-2.474
235	247.965	-17.926	-67.243	-2.124
240	254.179	-16.671	-61.957	-1.801
245	260.254	-15.385	-56.653	-1.505
250	266.189	-14.069	-51.336	-1.235
255	271.981	-12.723	-46.007	-0.991
260	277.629	-11.349	-40.671	-0.775
265	283.131	-9.947	-35.330	-0.585
270	288.488	-8.518	-29.988	-0.421
275	293.699	-7.063	-24.646	-0.285
280	298.764	-5.581	-19.308	-0.175
285	303.686	-4.075	-13.977	-0.092
290	308.465	-2.545	-8.654	-0.035
295	313.103	-0.991	-3.341	-0.005
300	317.603	0.586	1.960	-0.002
305	321.968	2.185	7.245	-0.025
310	326.202	3.806	12.515	-0.074
315	330.308	5.447	17.768	-0.150
320	334.290	7.108	23.001	-0.252
325	338.154	8.790	28.214	-0.380
330	341.906	10.490	33.405	-0.534
335	345.551	12.208	38.574	-0.714
340	349.096	13.945	43.720	-0.920
345	352.547	15.699	48.842	-1.151
350	355.912	17.470	53.938	-1.408
355	359.199	19.258	59.010	-1.690
360	362.417	21.062	64.057	-1.998
365	365.574	22.882	69.077	-2.331
370	368.680	24.718	74.072	-2.689
375	371.745	26.569	79.042	-3.072
380	374.779	28.435	83.986	-3.479
385	377.793	30.317	88.904	-3.911
390	380.798	32.213	93.799	-4.368
395	383.807	34.125	98.669	-4.849

$$\Delta_f H_m^\circ(C_{10}H_9O_5N_3, s) = -(667.31 \pm 11.02) kJ \cdot mol^{-1}$$

The $\Delta_f H_m^\circ(CO_2, g) = -393.51 \pm 0.13 kJ \cdot mol^{-1}$ and $\Delta_f H_m^\circ(H_2O, l) = -285.83 \pm 0.04 / kJ \cdot mol^{-1}$ were obtained from Refs. [36,37]

3.3. Optimized molecular geometry

Optimized geometrical parameters for $C_{10}H_9O_5N_3$ were calculated by using DFT method with B3LYP/6-31G (d,p) basis set, and calculated bond lengths/bond angles were listed in Table S2-S3.

Table 3

The constant-volume energy of combustion for $C_{10}H_9O_5N_3$ at 298.15 K and 0.1 MPa.

No	Sample mass, W/g	heat value of nickel wire, Q_{Ni}/J	heat value of nitric acid, Q_{HNO_3}/J	Corrected temperature rise, $\Delta_c T/K$	Combustion energies, $-\Delta_c U_i^{\circ}/J \cdot g^{-1}$
1	0.70028	38.0744	52.411956	0.903339	18064.30636
2	0.67954	35.1456	46.66818	0.877103	18083.87525
3	0.67577	36.02424	43.07832	0.877647	18200.14699
4	0.6921	35.73136	46.66818	0.905151	18326.42836
5	0.67534	39.5388	44.87325	0.869067	18024.67405
6	0.7685	38.0744	49.540068	1.001648	18268.68411

Average. $-\Delta_c U^{\circ} = \bar{x} \pm \sigma_a$

From the structural data given in the Tables, it is observed that all carbon–carbon bond lengths of the phenyl ring fall in the range of 1.390–1.403 Å for calculation and are observed in the range of 1.352–1.401 Å for single crystal XRD data. The selected some bond lengths, C(7)-N(2), N(2)-N(3), C(4)-C(7), C(8)-N(3) and C(1)-N(1), are observed as 1.374 Å, 1.378 Å, 1.480 Å, 1.273 Å and 1.472 Å, and calculated as 1.396 Å, 1.351 Å, 1.503 Å, 1.287 Å and 1.476 Å, respectively. The selected some bond angles, C(6)-C(1)-C(2), C(3)-C(4)-C(5), N(2)-C(7)-C(4), C(7)-N(2)-N(3), C(8)-N(3)-N(2) and N(3)-C(8)-C(10), are observed as 122.8°, 119.3°, 116.2°, 117.8°, 117.4° and 113.8°, whereas these values are calculated as 122.3°, 119.7°, 114.5°, 119.5°, 119.7° and 114.1°, respectively. The calculated values are in good agreement with the experimental data. The torsion angle, C(5)-C(4)-C(7)-N(2), is observed as 27.2° for theoretically, and calculated as 14.4° for experimentally, the deviation may be attributed to the intermolecular interactions and the interaction of hydrogen bonds between O(3) and O(6) in the crystal structure. The optimized molecular structure of the title compound is shown in Fig. S2.

3.4. Frontier molecular orbital (FMO) analysis

The energies of the highest occupied molecular orbital (HOMO) and the lowest unoccupied molecular orbital (LUMO) were investigated by using the DFT method at B3LYP/6-31G(d,p) level. The 3D plot of FMO of $C_{10}H_9O_5N_3$ has been drawn in Fig. 2. As shown in Fig. 2, the positive phase is presented in red and the negative one is in green. The HOMO is located over the acyl group and the LUMO is located over the benzene ring, which show that charges transfer occurs in the molecule. The computed energy values of HOMO and LUMO are -7.622 eV and -3.169 eV, respectively. The energy gap value of $C_{10}H_9O_5N_3$ molecule is 4.453 eV in gas phase. The HOMO energy describes the ability of giving electron, LUMO energy characterizes the ability of accepting electron, and the energy gap value is correlated with difficulty of electrons are excited from the ground state to excited state.

3.5. Molecular electrostatic potential (MEP) analysis

The MEP is a useful property to study the attacking sites for electrophilic and nucleophilic substitution reactions [38,39]. The different values of the electrostatic potential at the surface are represented by different colors. Red color represents regions of most negative electrostatic potential, and blue color signifies region of the most positive electrostatic potential. In order to predict reactive sites for electrophilic and nucleophilic attack for the title molecule. The MEP contour map of $C_{10}H_9O_5N_3$ is illustrated in Fig. 3. Fig. 3 shows that the oxygen atoms possess large negative potential, and the hydrogen atom bonding with nitrogen atom possesses large positive potential, of which due to the strong electron-withdrawing property of nitro, carbonyl, and carboxy group. Thus, it would be predicted that an electrophile would preferentially attack the oxygen atoms and nucleophilic preferentially

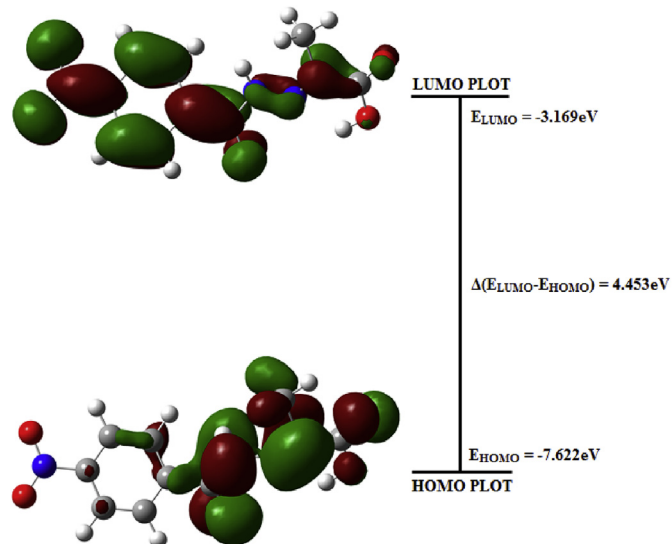


Fig. 2. The 3D plots of the frontier molecular orbital for $C_{10}H_9O_5N_3$.

attack the hydrogen atom attached to nitrogen atom.

4. Conclusion

In summary, we have synthesized a Schiff base compound $C_{10}H_9O_5N_3$. The Low-temperature heat capacity curve increases with increasing temperature from 78 K to 400 K, which shows that the structure of the $C_{10}H_9O_5N_3$ molecule is stable in the whole temperature region. The smoothed molar heat capacities and the thermodynamic functions of the $C_{10}H_9O_5N_3$ are derived from the thermodynamic equations. The standard molar enthalpy of formation of $C_{10}H_9O_5N_3$ is $\Delta_f H_m^{\circ} (C_{10}H_9N_3O_5, s) = -(667.31 \pm 11.02) \text{ kJ} \cdot \text{mol}^{-1}$. Additionally, the geometry of the title compound is optimized with the DFT method and the theoretical structural parameters are in good agreement with the single crystal XRD data.

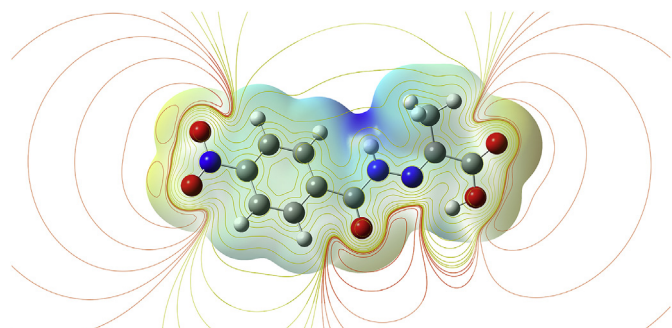


Fig. 3. The contour map of Molecular electrostatic potential surface for $C_{10}H_9O_5N_3$.

Frontier molecular orbital analysis shows that $E_{\text{HOMO}} = -7.622$ eV, $E_{\text{LUMO}} = -3.169$ eV and $\Delta(E_{\text{LUMO}}-E_{\text{HOMO}}) = 4.453$ eV. HOMO and LUMO occupy different locations of molecular structure of $C_{10}H_9O_5N_3$, which indicate that the charges transfer take place within the molecule. MEP analysis results reveal that electrophile would preferentially attack the O position, and nucleophilic preferentially attack the N–H position. The expected results are achieved by this research, as similar studies have been widely reported in the literature [40–43].

Acknowledgments

This work is supported by the National Natural Science Foundation of China (No. 21873063, 21273171 and 21703135), the Nature Science Foundation of Shaanxi Province (No. 2016JM2026 and 2018JQ2039), Special Research Project of Education Department of Shaanxi Provincial Government (No. 15JK1217, 17JS034 and 17JK0242), the Foundation of Shangluo (No. 16SKY005), the technology plan projects of Shangluo University (No. 17SKY027) and the National Demonstration Center for Experimental Chemistry Education (Northwest University).

Appendix A. Supplementary data

Supplementary data to this article can be found online at <https://doi.org/10.1016/j.molstruc.2019.02.050>.

References

- [1] B.S. Holla, M. Mahalinga, M.S. Karthikeyan, B. Poojary, P.M. Akberali, N.S. Kumari, *Eur. J. Med. Chem.* 40 (2005) 1173.
- [2] C.F. Qiao, L. Sun, S. Zhang, Q. Wei, C.S. Zhou, G. Xie, S.P. Chen, X.W. Yang, S.L. Gao, *Polyhedron* 119 (2016) 445.
- [3] N.O. Mahmoodi, M. Namroodi, F.G. Pirbasti, H. Roohi, I. Nikokar, *Res. Chem. Intermed.* 42 (2016) 3625.
- [4] L.W. Zheng, L.L. Wu, B.X. Zhao, W.L. Dong, J.Y. Miao, *Bioorg. Med. Chem.* 17 (2009) 1957.
- [5] R.M. Mohareb, R.A. Ibrahim, H.E. Moustafa, *Open Org. Chem. J.* 4 (2010) 8.
- [6] Y. Xia, C.D. Fan, B.X. Zhao, J. Zhao, D.S. Shin, J.Y. Miao, *Eur. J. Med. Chem.* 43 (2008) 2347.
- [7] N. Tabanca, D.E. Wedge, A. Ali, I.A. Khan, Z.A. Kaplancikli, M.D. Altintop, *Med. Chem. Res.* 22 (2013) 2602.
- [8] K. Takagi, H. Hamaguchi, T. Nishimatsu, T. Konno, *Vet. Parasitol.* 150 (2007) 177.
- [9] Z.B. Yang, D.Y. Hu, S. Zeng, B.A. Song, *Bioorg. Med. Chem. Lett.* 26 (2016) 1161.
- [10] V. Velezheva, P. Brennan, P. Ivanov, A. Kornienko, S. Lyubimov, K. Kazarian, B. Nikonenko, K. Majorov, A. Apt, *Bioorg. Med. Chem. Lett.* 26 (2016) 978.
- [11] A.K. Jordão, P.C. Sathler, V.F. Ferreira, V.R. Campos, M.C.B.V. De Souza, H.C. Castro, A. Lannes, A. Lourenco, C.R. Rodrigues, M.L. Bello, M.C.S. Lourenco, G.S.L. Carvalho, M.C.B. Almeida, A.C. Cunha, *Bioorg. Med. Chem.* 19 (2011) 5605.
- [12] J. Patole, U. Sandbhor, S. Padhye, D.N. Deobagkar, C.E. Anson, A. Powell, *Bioorg. Med. Chem. Lett.* 13 (2003) 51.
- [13] G. Gürkök, T. Coban, S. Suzen, *J. Enzym. Inhib. Med. Chem.* 24 (2009) 506.
- [14] H.S. Kareem, A. Ariffin, N. Nordin, T. Heidelberg, A. Abdul-Aziz, K.W. Kong, W.A. Yehye, *Eur. J. Med. Chem.* 103 (2015) 497.
- [15] K. Paulrasu, A. Duraikanu, M. Palrasu, A. Shanmugasundaram, M. Kuppusamy, B. Thirunavukkarasu, *Org. Biomol. Chem.* 12 (2014) 5911.
- [16] S.M. Soliman, J.H. Albering, M. Farooq, M.A.M. Wadaan, A. El-Faham, *Inorg. Chim. Acta* 466 (2017) 16.
- [17] P. Sathyadevi, P. Krishnamoorthy, R.R. Butorac, A.H. Cowley, N. Dharmaraj, *Metall* 4 (2012) 498.
- [18] M.K.M. Subarkhan, R. Ramesh, *Inorg. Chem. Front.* 3 (2016) 1245.
- [19] K.M. Ibrahim, I.M. Gabr, G.M.A. El-Reash, R.R. Zaky, *Monatsh. Chem.* 140 (2009) 625.
- [20] C. Li, L. Wang, *Transition Met. Chem.* 24 (1999) 206.
- [21] P. Krishnamoorthy, P. Sathyadevi, K. Senthilkumar, P.T. Muthiah, R. Ramesh, N. Dharmaraj, *Inorg. Chem. Commun.* 14 (2011) 1318.
- [22] Y.P. Liu, Y.Y. Di, W.Y. Dan, D.H. He, Y.X. Kong, W.W. Yang, *J. Therm. Anal. Calorim.* 103 (2011) 987.
- [23] V.N. Emel'yanenko, A.V. Yermalayeu, M. Voges, C. Held, G. Sadowski, S.P. Verevkin, *Fluid Phase Equilib.* 422 (2016) 99.
- [24] J.P. O'Connell, R. Gani, P.M. Mathias, G. Maurer, J.D. Olson, P.A. Crafts, *Ind. Eng. Chem. Res.* 48 (2009) 4619.
- [25] O. Pfohl, R. Dohrn, *Fluid Phase Equilib.* 217 (2004) 189.
- [26] W.E. Hatton, D.L. Hildenbrand, G.C. Sinke, D.R. Stull, *J. Chem. Eng. Data* 7 (1962) 229.
- [27] M.A. White, *Spectrochim. Acta* 74 (1984) 55.
- [28] W.W. Yang, Y.Y. Di, Y.X. Kong, Y.F. Zhu, Z.C. Tan, *J. Chem. Eng. Data* 54 (2009) 2038.
- [29] J.M. Seminario, P. Politzer, *Modern Density Functional Theory: a Tool for Chemistry*, Elsevier, New Orleans, 1995.
- [30] J. Lukose, C.Y. Panicker, P.S. Nayak, B. Narayana, B.K. Sarojini, C. Van Alsenoy, A.A. Al-Saadi, *Spectrochim. Acta* 135 (2015) 608.
- [31] K. Fukui, T. Yonezawa, H. Shingu, *J. Chem. Phys.* 20 (1952) 722.
- [32] S. Muthu, S. Renuga, *Spectrochim. Acta* 118 (2014) 683.
- [33] G. Subhapriya, S. Kalyanaraman, N. Surumbarkuzhal, S. Vijayalakshmi, V. Krishnakumar, *J. Mol. Struct.* 1083 (2015) 48.
- [34] A. Jamadar, A.K. Duhme-Klair, K. Vemuri, M. Sritharan, P. Dandawate, S. Padhye, *Dalton Trans.* 41 (2012) 9192.
- [35] M.A.V. Ribeiro da Silva, M.A.R. Matos, C.M.A. Do Rio, *J. Chem. Thermodyn.* 29 (1997) 901.
- [36] J.D. Cox, J. Drowart, L.G. Hepler, V.A. Medvedev, D.D. Wagman, CODATA recommended key values for thermodynamics, 1977 Report of the CODATA Task Group on key values for thermodynamics, *J. Chem. Thermodyn.* 10 (1978) (1977) 903.
- [37] J.D. Cox, D.D. Wagman, V.A. Medvedev, CODATA Key Values for Thermodynamics, vol. 1, Hemisphere Pub. Corp., New York, 1989, p. 138.
- [38] J.S. Murray, K. Sen, *Molecular Electrostatic Potentials, Concepts and Applications*, Elsevier, Amsterdam, 1996.
- [39] P. Politzer, D.G. Truhlar, *Chemical Application of Atomic and Molecular Electrostatic Potentials*, Plenum, New York, 1981.
- [40] Z.J. Wang, S.P. Chen, Q. Yang, S.L. Gao, *J. Chem. Eng. Data* 55 (2010) 2558.
- [41] X. Li, J.H. Jiang, H.W. Gu, S.X. Xiao, C.H. Li, L.J. Ye, X. Li, Q.G. Li, F. Xu, L.X. Sun, *J. Therm. Anal. Calorim.* 119 (2015) 721.
- [42] A.K. Srivastava, B. Narayana, B.K. Sarojini, N. Misra, *Indian J. Phys.* 88 (2014) 547.
- [43] M.S. Alam, D. Lee, *Spectrochim. Acta* 145 (2015) 563.